JOURNAL OF SOLID STATE CHEMISTRY 24, 21–31 (1978)

High-Resolution Crystal Structure Images of Beta Phase ($Pr_{24}O_{44}$) in the Praseodymium Oxide System*

EDWARD SUMMERVILLE,† RICHARD T. TUENGE, AND LEROY EYRING‡

Department of Chemistry, Arizona State University, Tempe, Arizona 85281

Received July 25, 1977

Crystal structure images of the beta phase in the praseodymium oxide system are presented. A structural model for $Pr_{24}O_{44}$ is developed which involves chemical twining of a primitive triclinic unit cell ($Pr_{12}O_{22}$) in different ways, resulting in two possible polymorphs. Crystal structure images of the beta phase are compared with calculated images of one of the possible polymorphs and diffraction effects from this polymorph are shown to be compatible with those observed. A general structural principle is suggested which may be common to all intermediate phases in the binary rare earth oxide systems.

Introduction

In a previous article (*1*) an attempt was made to correlate calculated *n*-beam crystal structure images with observed images for a fluorite-related phase with known structure, namely, M_7O_{12}. Although there appears to be no correlation between the actual structure and the observed image under the circumstances of that investigation (i.e., crystal thicknesses greater than 100 Å) the calculated and observed images were very similar. It was therefore proposed to attempt to determine the structure of another member of the homologous series of fluorite-related phases, the beta phase ($Pr_{12}O_{22}$), by comparing the observed electron microscope images with those calculated from plausible models. The explicit assumption made is that the better the agreement between the observed images and those calculated for a particular model the more likely the structure is to be the correct one.

It will be shown here that under certain conditions the observed images for beta phase do indeed correspond to the projected charge density of the proposed structural model. The one-to-one correlation between structural features and electron micrograph contrast is necessary to ensure that the proposed model is in fact the correct structure for the phase. This will be illustrated here by comparing the variety of images of this phase that can be observed under various conditions of specimen and instrument with the large number of different patterns resulting from calculations for a particular model.

The unit cells of members in the R_nO_{2n-2} homologous series of fluorite-related rare earth oxides have been described by Kunzmann and Eyring (*2*) (see Fig. 1) and a structural model which would apply to the odd-membered phases was proposed. It will be shown in this paper that it may also apply to the even-numbered phases of the homologous series.

* Work supported by the United States Energy Research and Development Administration.

† Present address: School of Physical Sciences, Flinders University of South Australia, Bedford Park 5042, South Australia.

‡ Author to whom inquiries should be addressed.

0022–4596/78/0241–0021$02.00/0

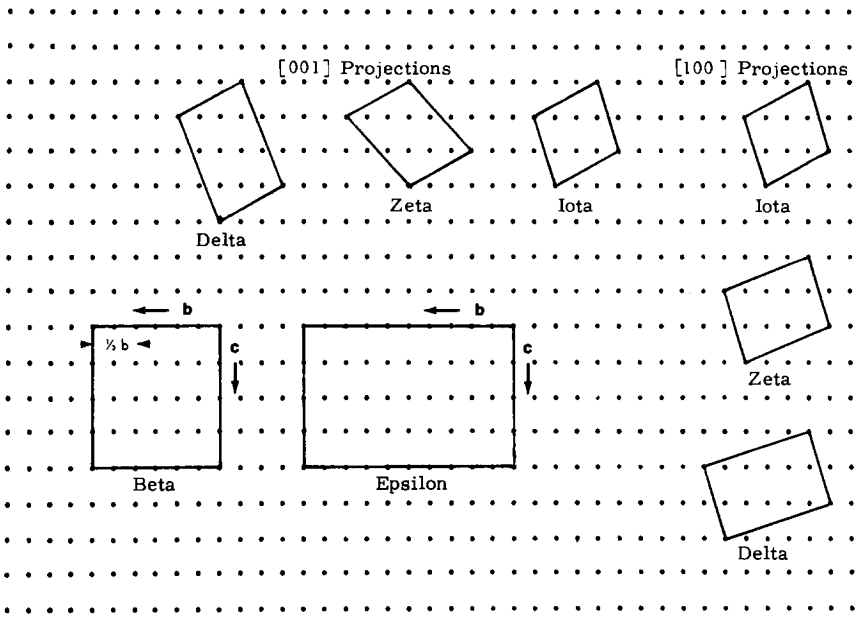

FIG. 1. Projections of the unit cells of each of the intermediate phases down $[211]_F$. Eclipsed rows of ideal cation sites are represented as dots.

Experimental

All relevant experimental techniques have been described previously (*1*).

Results and Discussion

Structural Information for ($Pr_{12}O_{22}$)

The most convenient (though nonreduced) unit cell of beta phase has been described (*3*) as being monoclinic, space group $P2_1/n$ and having axial relationships equivalent to

$$\mathbf{a} = \mathbf{a}_1 + \tfrac{1}{2}\mathbf{a}_2 - \tfrac{1}{2}\mathbf{a}_3,$$
$$\mathbf{b} = +\tfrac{3}{2}\mathbf{a}_2 + \tfrac{3}{2}\mathbf{a}_3,$$
$$\mathbf{c} = -2\mathbf{a}_2 + 2\mathbf{a}_3,$$

and these axial relationships will be retained in this discussion. The systematic absences of this space group and their cause are:

$0k0$	$k = 2n + 1$	2_1- axis
$h0l$	$h + 1 = 2n + 1$	n-glide

The existence of the screw axis cannot be verified by electron diffraction because of dynamical diffraction effects; however, the existence of the glide plane would be evident in a $\langle 010 \rangle_{12}$ diffraction pattern (numerical subscripts refer to the value of "n" in the homologous series M_nO_{2n-2}; the subscript F will designate the fluorite subcell). Examination of many $\langle 010 \rangle_{12}$ diffraction patterns showed that absences resulting from the glide plane occurred in some instances; however, in many other cases sharp, very weak reflections were present. These additional reflections could have resulted from the presence of a very small proportion of a twin orientation or they may indicate that the glide plane is only approximate.

Reexamination of the single-crystal X-ray data referred to by Kunzmann and Eyring (*2*) showed the occurrence of many absences of the form

$$h + (k/3) + 1 = 2n + 1.$$

About three-fourths of 360 such reflections were absent and only about 12 were of moderate intensity. These absences are important for two reasons: (1) when $k = 0$ the rule

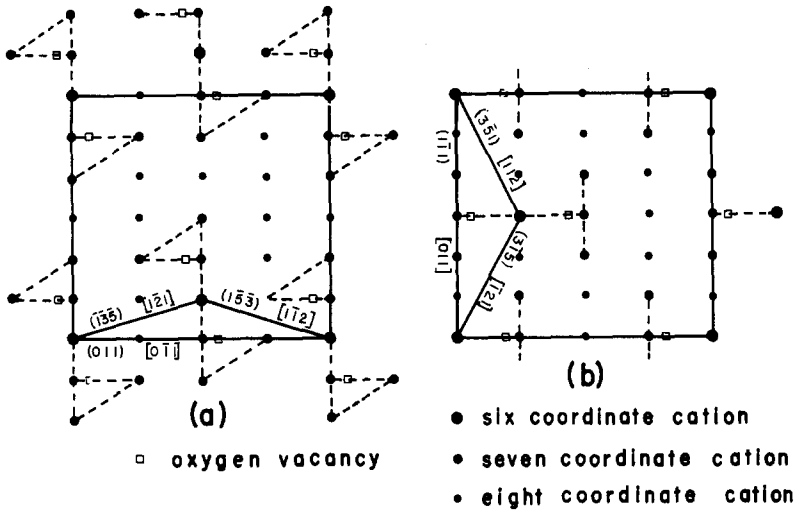

FIG. 2. Diagrammatic representations of the proposed structures of the beta phase. (a) Model with symmetry $P1$. (b) Model with symmetry Pm.

predicts the same absences as would result from an n-glide, and (2) if the rule were strictly obeyed it would indicate that the unit cell would be "one-third body-centered along the b-axis." Consequently, if the unit cell is subdivided into three units such that for each $a = a_\beta$, $b = \frac{1}{3}b_\beta$, $c = c_\beta$, these units would be body-centered. As can be seen from Fig. 1, in the ideal beta phase unit cell (i.e., ignoring the existence of anion vacancies) each of these units is body-centered. This raises the further possibility that the "systemmatic absences," attributed to the n-glide, are accidental "absences" resulting from the high pseudosymmetry of the fluorite subcell. Since the ideal beta phase cell has the n-glide and since it is approximately one-third body-centered, the observed set of absences would result if these symmetry elements are not significantly destroyed during the ordering process. If this is the case the absences imply nothing about the space group of this phase.

Structural Models

Two proposed models for the structure of beta phase are shown in projection down the a-axis in Fig. 2. The one having space group $P1$ shown in Fig. 2a, has been studied in detail. It consists of cation octahedra located at the origin and at $\frac{1}{2}, \frac{1}{6}, \frac{1}{2}$. (The term "cation octahedra" is used to designate near-octahedral anion coordination polyhedra resulting from the loss of two oxygen atoms from the body diagonal of an MO_8 coordination cube. The terms "cation" and "anion" are used for convenience and imply nothing about the charges on atomic species.) The anion vacancies are arranged as shown and occur across the body diagonal of an MO_8 cube (as in iota). The vectors from the cation octahedra on each of the four origins at the bottom of the figure to the octahedral cation at $\frac{1}{2}, \frac{1}{6}, \frac{1}{2}$ are all $\frac{1}{2}[211]_F$ vectors. Thus the unit cell can be divided into two halves, each of which is an $n = 12$ version of the odd-membered series described by Kunzmann and Eyring (*2*). On the other hand this structure can be described as consisting of slabs of fluorite (PrO_2) alternating with slabs of iota-like (Pr_7O_{12}) material being arranged perpendicular to a $[110]_F$ axis (the b-axis of the beta phase).

The second proposed model having symmetry Pm, Fig. 2b, is structurally very similar. It consists of cation octahedra at the origin and at $\frac{1}{2}, \frac{1}{2}, \frac{1}{4}$. The anion vacancies again occur

TABLE I

AXIAL RELATIONSHIPS FOR THE REAL AND PROPOSED PRIMITIVE UNIT-CELLS OF BETA ($Pr_{24}O_{44}$)

"Monoclinic" ($n = 24$)			$P1$ ($n = 12$)			Pm ($n = 12$)		
a_F	b_F	c_F	a_F	b_F	c_F	a_F	b_F	c_F
1	$\frac{1}{2}$	$-\frac{1}{2}$	1	$\frac{1}{2}$	$-\frac{1}{2}$	1	$\frac{1}{2}$	$-\frac{1}{2}$
0	$\frac{3}{2}$	$\frac{3}{2}$	0	$\frac{3}{2}$	$\frac{3}{2}$	$\frac{1}{2}$	$\frac{1}{2}$	1
0	2	2	$\frac{1}{2}$	$-\frac{1}{2}$	1	0	2	2

across the body diagonal of an MO_8 cube and again the vectors from all four left-hand origins to the $\frac{1}{2}, \frac{1}{2}, \frac{1}{4}$ site are each of the type $\frac{1}{2}[211]_F$. As before, the structure can be described in terms of chemical twinning of an $n = 12$ triclinic unit cell, or as slabs of iota-like material separated by slabs of fluorite, but in this latter case the slabs are perpendicular to a $[111]_F$ axis. The axial relationships of these two $n = 12$ triclinic cells and of the $n = 24$ "monoclinic" cell are given in Table I.

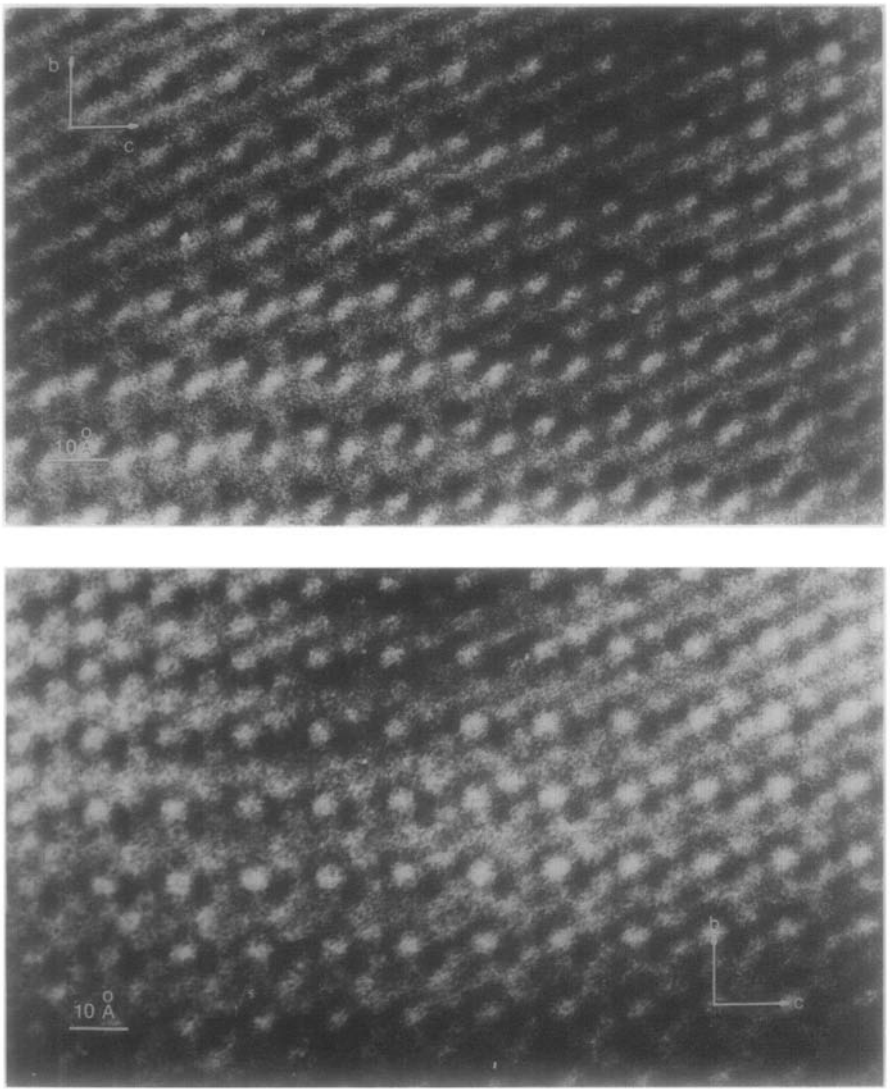

FIG. 3. Crystal structure images of beta from a $\langle 100 \rangle_{12} \equiv \langle 21\bar{1} \rangle_F$ zone.

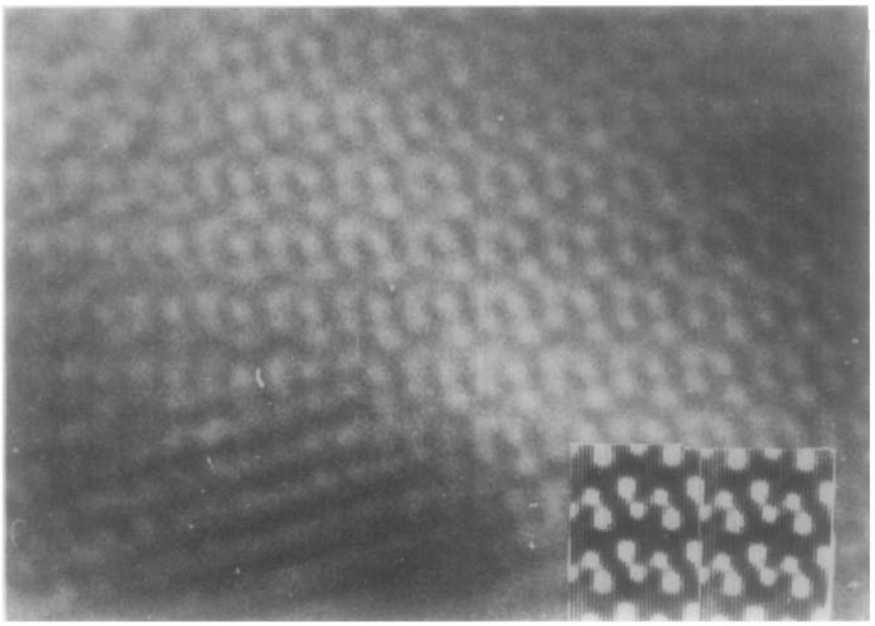

FIG. 4. Crystal structure $\langle 211 \rangle_F$ image of a thin beta-phase crystal. Inset is a calculated image from the *P*1 structural model.

Observed Images

Figure 3 shows $\langle 100 \rangle_{12}$ ($\langle 21\bar{1} \rangle_F$) images of beta phase typically observed with the high-resolution electron microscope. These images were obtained from two crystal fragments of different and undetermined thicknesses.

Figure 4 displays a crystal structure image from a $\langle 100 \rangle_{12}$ zone of beta phase obtained from near the edge of a thin crystal fragment, however, the crystal thickness is not known. The image was recorded by using an objective aperture of 0.308 $Å^{-1}$ and a defocus value of about −900 Å. The divergence of the illumination was 0.9×10^{-3} rad. The striking similarity between the pairs of white spots in this image and the position of the projected vacancies in the *P*1 model (Fig. 2a) suggests an intuitive interpretation where the image contrast represents the projected potential of this phase. The calculated image is superimposed on the lower right-hand corner to emphasize the great similarity.

A crystal structure image from a $\langle 010 \rangle_{12}$ ($\equiv \langle 110 \rangle_F$) zone of beta is shown in Fig. 5a. The spot array corresponds precisely to the projection of the cation octahedra sites of the *P*1 structure down this direction as shown in Fig. 5b.

Calculated Images

In order to test the acceptability of the proposed *P*1 model of the beta phase calculations of image intensities were made by use of the slice method of Goodman and Moodie (*4*) based on the *n*-beam dynamical theory of Cowley and Moodie (*5*). The atomic positions were predicted for this model by comparison with the structure of Pr_7O_{12} and then the diffraction pattern and images of the structure were calculated using the programs FCOEFF and DEFECT written by Skarnulis (*1*). To accomplish this a transformation matrix was derived to convert the known iota-phase cation positions to those of beta. This matrix was then applied to each of the six seven-coordinated cations surrounding every vacancy pair. Anion positions were not altered since their positions in iota probably do not correlate well with their positions in beta (due to the absence of strings of six-coordinated cations in

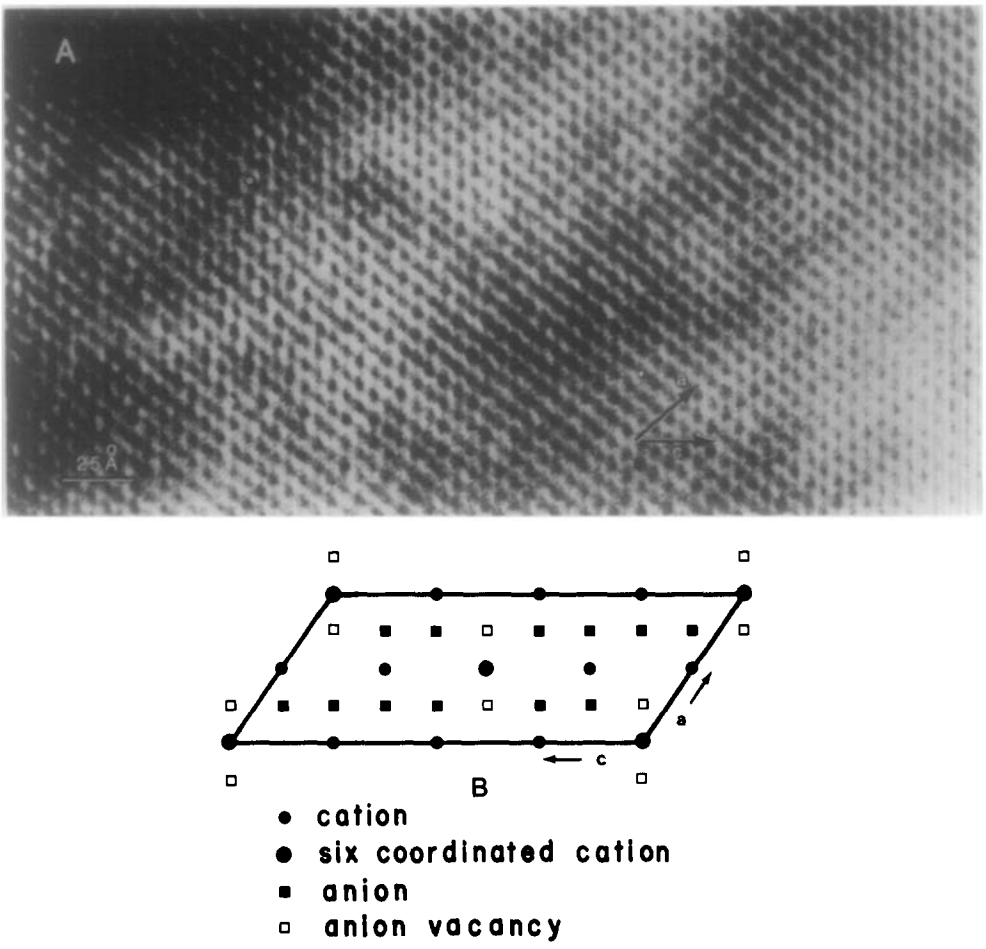

FIG. 5. (a) $\langle 010 \rangle_{12}$ crystal structure image of beta. (b) Diagram of the arrangement of cation octahedra corresponding to the crystal structure image in Fig. 5a.

the latter structure). Proposed vacancy sites were of course left vacant. The resulting positional parameters listed in Table II were input to FCOEFF and DEFECT. The slice thickness for the calculations was the a-axis length of 6.87 Å. The experimental parameters used for the calculation were a spherical aberation constant $C_s = 1.8$ mm, half-width of depth-of-focus Gaussian of 120 Å, objective aperture of 0.285 $Å^{-1}$, and divergence angle of 0.9×10^{-3} rad; 937 beams were used in the multislice calculation. The resulting diffraction intensities are given in Table III.

The calculated diffraction patterns show "absences" consistent with one-third body-centering (and also of an n-glide) despite the fact that the structure has no symmetry. This effect is partly due to the fact that 12 of the cations and the 44 anions are still on normal fluorite sites, but 12 cations have been shifted as in the iota phase and 4 anions have been removed without producing diffraction effects in gross disagreement with the observed pattern. Provided the remaining atomic shifts are reasonably compatible with one-third body centering it seems quite possible that this structure could completely satisfy the observed diffraction pattern of the beta phase.

Figure 6 shows a series of n-beam crystal structure images in projection down the a-axis.

TABLE II

ATOM POSITIONS FOR THE *P*1 MODEL OF BETA ($Pr_{12}O_{22}$)[a]

Pr No.	*x*	*y*	*z*	Pr No.	*x*	*y*	*z*
1	0.000	0.000	0.000	13	0.500	0.500	0.000
2	0.969	0.996	0.234	14	0.500	0.500	0.750
3	0.978	0.993	0.505	15	0.490	0.518	0.500
4	0.000	0.000	0.750	16	0.500	0.500	0.250
5	0.522	0.174	0.995	17	0.010	0.648	0.000
6	0.500	0.167	0.750	18	0.000	0.667	0.250
7	0.500	0.167	0.500	19	0.000	0.667	0.500
8	0.531	0.171	0.266	20	0.000	0.667	0.750
9	0.990	0.351	0.000	21	0.478	0.826	0.005
10	0.000	0.333	0.250	22	0.469	0.829	0.734
11	0.022	0.341	0.495	23	0.510	0.815	0.500
12	0.031	0.338	0.766	24	0.500	0.833	0.250

Vacancy No.	*x*	*y*	*z*
1	0.250	0.167	0.063
2	0.250	0.000	0.063
3	0.750	0.833	0.938
4	0.750	0.333	0.563

[a] Anion positions used were all ideal fluorite positions.

Variation of the images with defocus is shown across the top and variation with specimen thickness down the side. The origin is located at the lower left-hand corner of each image with three unit cell repeat distances in the *c*-direction and two repeat distances in the *b*-direction. It can be seen that images calculated for thicknesses 27 and 54 Å over a defocus range of −800 to −1000 Å correspond directly to the projected structure (white spots occur at positions of oxygen vacancies with four vacancies per unit cell). This correlation was previously observed in the calculated images of the iota (M_7O_{12}) phase; however, in the present case this correlation reoccurs for thicker crystals (162 Å). This repetition of thin-crystal (<54 Å) images at greater thickness has been observed for ReO_3-related block structures by Fejes *et al.* (*6*). Calculated images of beta phase at other thicknesses show a variety of contrast patterns; some approximate the thin-crystal image and others show no structural relationship. The images contain anywhere from one to five bright spots per cell.

It can be seen that there is an excellent agreement between the observed thin-crystal image of beta phase (Fig. 4) and the calculated thin-crystal images. This confirms the contention that the experimental image shown in Fig. 4 represents the projected potential of the crystal. However, the thickness of the crystal which produced this image may in fact be 150–170 Å rather than 50 Å. Although the actual thicknesses of the fragments is not known, crystals of the fluorite-related rare earth oxides do not cleave well and regions as thin as 50 Å may be very rare. There is also a close correspondence between images calculated at other thicknesses which do not represent the projected potential and some observed images (e.g., Fig. 3 and the image calculated at 270 Å thick and −1200 Å defocus), providing further evidence for the *P*1 model for the structure of beta phase. Any disagreement can be rationalized as resulting from inaccu-

TABLE III

CALCULATED DIFFRACTION PATTERN FOR THE *P*1 MODEL OF BETA ($Pr_{12}O_{22}$)

"Absences"		$\langle 100 \rangle_{12}$ ZONE Reflections	
h k l	$\lvert F \rvert^2$	*h k l*	$\lvert F \rvert^2$
0 0 1	0.003[a]	0 1 0	113
0 0 3	0.924[a]	0 1 1	23
0 3 0	0.034[b]	0 2 0	12
0 3 2	0.013[b]	0 2 1	190
0 3 4	0.035[b]	0 1 2	43
0 6 1	0.155[b]	0 2 2	17
0 6 3	0.246[b]	0 3 1	105
		$\langle 010 \rangle_{12}$ Zone	
h k l[a]	$\lvert F \rvert^2$[a]	*h k l*	$\lvert F \rvert^2$
0 0 1	0.003	0 0 2	16.8
0 0 3	0.024	0 0 4	33,681.9
0 0 5	0.043	0 0 6	48.1
1 0 0	0.000	1 0 1	187.9
1 0 2	0.009	1 0 3	60.7
1 0 4	0.023	1 0 5	279.9
1 0 6	0.031	2 0 2	39.6
2 0 1	0.002	2 0 4	9765.8
2 0 3	0.010	2 0 6	15.5
2 0 5	0.016		

[a] Expected from an *n*-glide or one-third body centering.

[b] Expected only from one-third body centering.

racies in the predicted atomic positions. Not only are many atoms on ideal fluorite sites but those shifts which have been made to atomic positions are unlikely to be correct even if the model is correct. In particular, for the *P*1 model, the real atom shifts along the *c*-axis are probably greater than those derived from the iota phase structure because the vacancy planes are further apart in beta than in iota. It could similarly be expected that the real atom shifts along the *b*-axis in the *Pm* model would be greater than those derived from the iota structure. No calculations have been performed utilizing these larger shifts because with so many variables it would appear to be possible to obtain any desired result without the shifted positions necessarily being correct. Considering these circumstances the agreement between the observed and calculated images is probably better than should have been anticipated. A structure very similar to the *P*1 structure above but with the anion vacancies near $\frac{1}{2}$, $\frac{1}{6}$, $\frac{1}{2}$ rotated 180° about an axis parallel to the *b*-axis has *Pn* symmetry. However, images calculated for this model show almost no correlation with those observed.

On Disorder in Beta ($Pr_{12}O_{22}$)

As the effective end member of the homologous series beta contains the lowest concentration of anion vacancies. If the proposed structural models are correct it seems reasonable to suppose that the ordering forces between the planes of six-coordinated cations would decrease as the vacancy concentration decreases and the spacing of these planes increases. Beta then could be substantially less-ordered than the other homologs. Figure 7 shows a case of an apparent stacking fault in which there appears to be a shift in the positions of the six-coordinated cations along the *b*-axis. There is some evidence that both polymorphs may be imaged in this figure. Another, less easily interpreted defect is shown in Fig. 8—in this case the positions of the spots do not change, only their intensities. The only reasonable explanation for this change appears to be that the *b*-axis on one side of the fault is in the opposite direction to the *b*-axis on the other side of the fault. If this is so then the two regions are acually twins, but the diffraction pattern of one twin will completely overlie that of the other. Several crystals of beta consisted of twin domains with an average diameter of about 200 Å. If the conclusions drawn on the several types of defects observed in beta phase are correct then the lack of success in refining the X-ray data is to be expected. Apart from conventional problems of mechanical twinning and multiple nucleation, some of the above forms of disorder would completely overlay those of others.

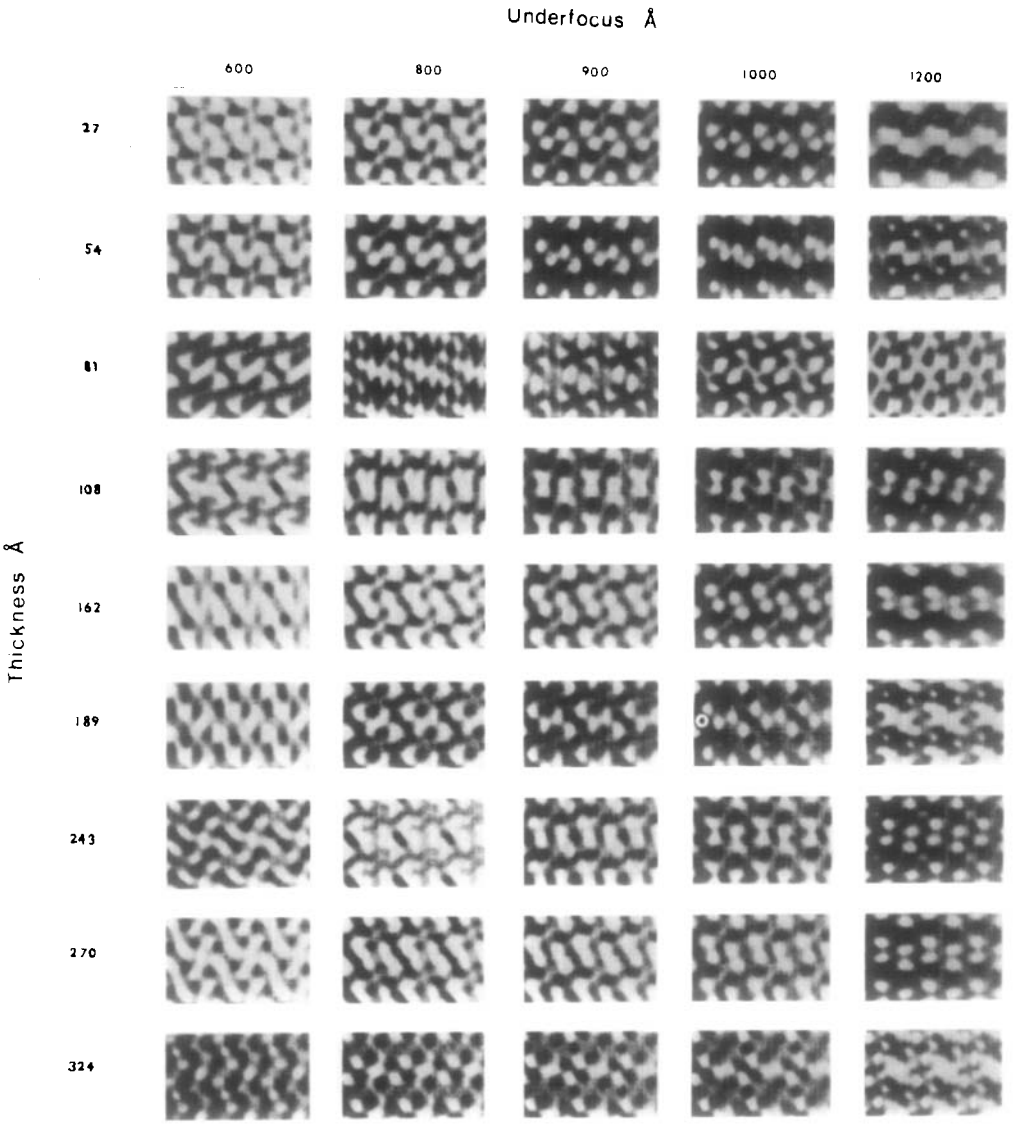

FIG. 6. Calculated $\langle 100 \rangle_{12}$ crystal structure images of the $P1$ model.

On the Absence of a Homolog with $n = 8$

Figure 9 shows the $n = 8$ structural analog of the proposed even-membered series of phases. In this case the cation octahedra approach each other such that one vacancy from each of two alternate cations occur across the body diagonal of an MO_8 cube of the intervening cation. This forms zig-zag strings of six-coordinated cations as in $Sr_4U_2O_{10}$ (*7*). The speculation can then be made that the lattice relaxations about one set of alternate cations are incompatible with those required about the set of intervening cations, resulting in destabilization of the phase. In iota this interference does not occur because of the offsetting of the cation octahedra.

Conclusions

On the basis of the proposed structure for the beta phase in the praseodymium oxide system it seems possible to extend the struc-

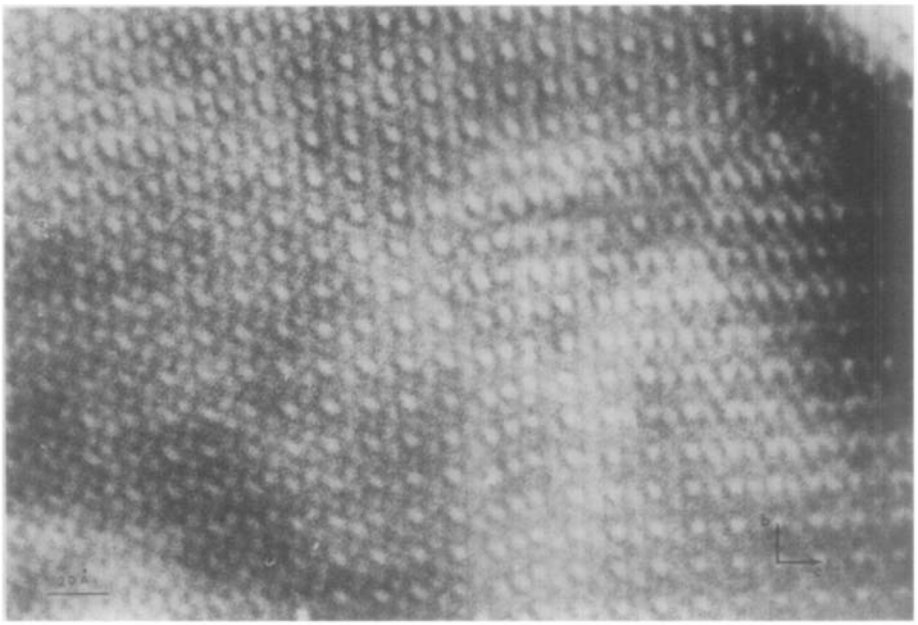

FIG. 7. Crystal structure image of beta from a $\langle 100 \rangle_{12}$ zone showing apparent stacking faults.

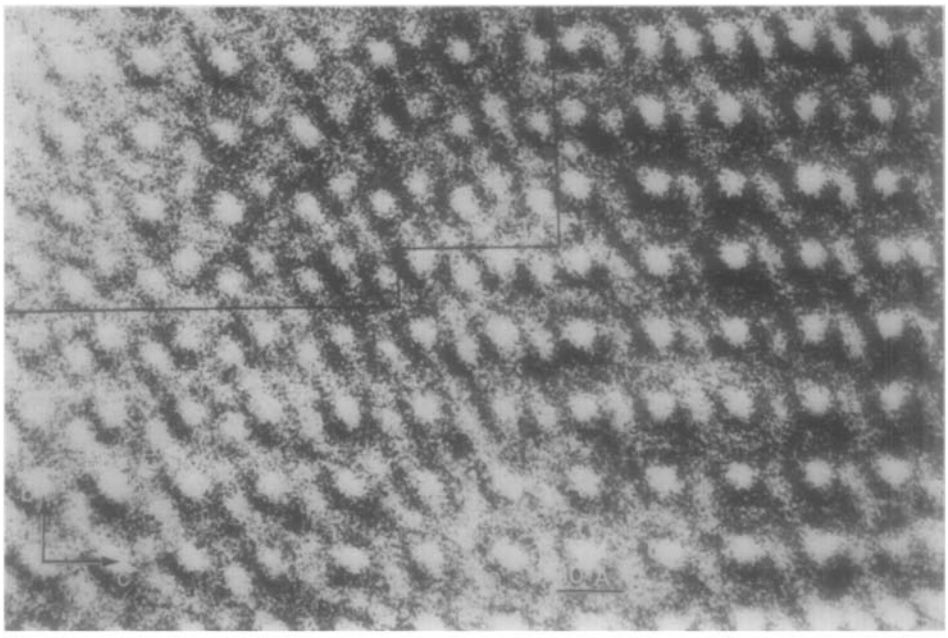

FIG. 8. Crystal structure images from $\langle 100 \rangle_{12}$ showing image variations which may correspond to domains of each of the proposed polymorphs of beta.

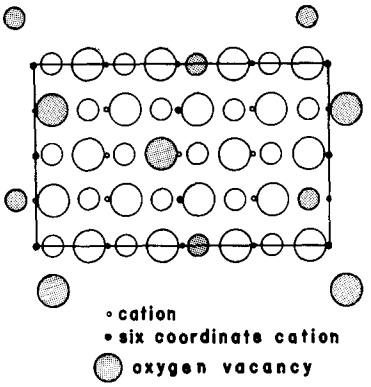

FIG. 9. Hypothetical structure for the missing M_8O_{14} phase showing the strings of six-coordinated cations parallel to $[100]_F$.

tural model proposed by Kunzmann and Eyring. (*2*). In each of the odd-membered phases the set of $(\bar{1}35)_F$ planes of cations has every *n*th plane composed entirely of six-coordinated cations. To be specific, in zeta (M_9O_{16}) every ninth $(\bar{1}35)_F$ plane of cations consists only of six-coordinated cations, in delta the same is true of every eleventh $(\bar{1}35)_F$ plane. The same principle apparently applies to the even-membered phases; however, the $\{135\}_F$ planes are puckered so that on average the six-coordinated cations lie on planes parallel to $(110)_F$. In the case of beta, for example, there are alternate segments of $(135)_F$ and $(5\bar{3}1)_F$ planes of six-coordinated cations which make up the *b*-face of the "monoclinic" unit cell. These average out to be the $(101)_F$ plane.

The proposed model makes a number of implications not suggested by previous models. It limits the range of the homologous series to values of *n* above six, so that Pr_2O_3 is not structurally $n = 4$ of the series, nor can there be structurally similar phases with $n = 5$ or 6. The possibility exists that the model can be used to rationalize the absence of the homolog with $n = 8$. Since beta is a typical member of the homologous series, no special structural significance is attached to it; hence the model predicts that higher homologs can exist and the fact that they have not been observed must then be attributed to kinetic effects.

While the proposed model for the beta phase shows good correlation with the available data, verification from structure refinement of intensity measurements is necessary.

Acknowledgment

The use of the CSSS High Resolution Microscopy Facility and the services of its manager, John C. Wheatley, are appreciated. In addition, the university provided the computer facilities needed for the image calculation for which we are grateful.

References

1. A. J. SKARNULIS, E. SUMMERVILLE AND L. EYRING, *J. Solid State Chem.*, in press.
2. P. KUNZMANN AND L. EYRING, *J. Solid State Chem.* **14**, 229–237 (1975).
3. M. Z. LOWENSTEIN, L. KIHLBORG, K. H. LAU, J. M. HASCHKE, AND L. EYRING (1972). *NBS Spec. Pub.* **364**, 344–351.
4. P. GOODMAN AND A. F. MOODIE, *Acta Crystallogr. A* **30**, 280–290 (1974).
5. J. M. COWLEY AND A. F. MOODIE, *Proc. Phys. Soc. B* **70**, 497–504 (1957).
6. P. L. FEJES, S. IIJIMA, AND J. M. COWLEY, *Acta Crystallogr. A* **29**, 710–714 (1973).
7. B. O. LOOPSTRA AND H. M. RIETVELD, *Acta Crystallogr. B* **25**, 787 (1969).